EGNOS Test Bed Ionospheric Corrections Under the October and November 2003 Storms

Manuel Hernández-Pajares, J. Miguel Juan Zornoza, Jaume Sanz Subirana, Richard Farnworth, and Santiago Soley

***Abstract*—Two severe geomagnetic storms were experienced on October 29–31 and November 20, 2003, degrading significantly the European Geostationary Navigation Overlay Service (EGNOS) Test Bed (ESTB) performance in Europe. Such storms reached extreme values of Kp $=$ 9 during the most severe periods. The analysis of the ESTB ionospheric corrections and their effect on the ESTB integrity and accuracy is presented in this work. The ESTB performance during those storms was monitored from a network of global positioning system (GPS) receivers widely distributed over Europe, including the ESTB reference stations, and the geographical degradation of the accuracy is analyzed in this paper. The correlation between the Kp index and the misleading information (MI) events is also shown. During the most severe stormy periods, the errors in the ESTB ionospheric corrections and its integrity bounds are analyzed to explain the peaks in the navigation system error, which produces MIs. This analysis has been carried out by comparing with direct dual-frequency GPS measurements and global ionospheric maps.**

***Index Terms*—EGNOS Test Bed (ESTB), European Geostationary Navigation Overlay Service (EGNOS), ionosphere, Satellite Based Augmentation System (SBAS), storm.**

I. Introduction

THE European Geostationary Navigation Overlay Service (EGNOS) Test Bed (ESTB) is a simple prototype of the final European Geostationary Navigation Overlay Service, developed by the European Space Agency as a tool for supporting EGNOS design and demonstration to users.[1]

The EGNOS System is the European Satellite Based Augmentation System (SBAS) equivalent to the U.S. Wide Area Augmentation System. With three geostationary satellites and a network of ground reference stations, this system transmits differential corrections and integrity data to enhance the positioning signals sent out by global positioning systems (GPS) and global navigation satellite systems, and make them suitable for safety-critical applications such as commercial aviation.

Manuscript received November 30, 2004; revised April 8, 2005. This work was supported in part by EUROCONTROL under Contract C/1.057/CE/JR/03 and in part by the Spanish Project ESP2004-05682-C02-01.

M. Hernández-Pajares and J. Sanz Subirana are with the Department of Applied Mathematics and Telematics, Universitat Politècnica de Catalunya, 08034 Barcelona, Spain (e-mail: manuel@ma4.upc.edu; jaume@ma4.upc.edu).

J. M. Juan Zornoza is with the Department of Applied Physics, Universitat Politècnica de Catalunya, 08034 Barcelona, Spain (e-mail: miguel@fa.upc.edu).

R. Farnworth and S. Soley are with the Eurocontrol Experimental Centre, F-91222 Bretigny, France (e-mail: richard.farnworth@eurocontrol.int; santiago.soley@pildo.com).

Digital Object Identifier 10.1109/TGRS.2005.855625

The ESTB, as a prototype of the EGNOS system, has several limitations. It works with a reduced number of reference stations (RIMS), about 12, compared to the 34 RIMS in EGNOS. In the ESTB, there is no function to check the integrity of the broadcast information, while in EGNOS there are two elements devoted to an integrity check: one within the EGNOS Central Processing Facility Processing Set (CPFPS) and the other on the complete EGNOS central processing check set (CPFCS). That is, the ESTB is an accuracy system with no integrity intended. However, running with a simple ionospheric algorithm, it provides a very good accuracy for a system of such low complexity.

The ionosphere is the component of the SBAS messages that is the most difficult to model. From a network of reference stations, with typical distances of hundreds of kilometers, vertical delays [total electron content (TEC)] and their integrity bounds are computed by the master station and provided to the users on a $5^\circ \times 5^\circ$ or $10^\circ \times 10^\circ$ grid (depending on the latitude) with a maximum update interval of 300 s.

Under normal conditions, the SBAS systems are capable of satisfying the aviation requirements for accuracy, integrity, availability, and continuity. But large disturbances in the ionosphere (storms and scintillation) can seriously affect the system performance.

Space weather disturbances such as solar flares, coronal holes, and coronal mass ejections are the main causes of geomagnetic storms on Earth, where ejections of charged particles (in solar wind) and electromagnetic energy propagate toward the Earth and couple the outer magnetosphere with the ionosphere and inner layers of the Earth's atmosphere. In such circumstances, smooth variations on TEC can be replaced by rapid fluctuations, and some regions experience significantly higher or lower TEC values than normal.

On October 28, 2003, an intense solar eruption (an X-flare) was detected in an active region which had grown to be one of the largest sunspots ever seen by the Solar Heliospheric Observatory (SOHO) satellite.[2] It appeared as a bright flash in the SOHO ultraviolet images. This sudden enhancement of the solar radiation in the X-ray and extreme ultraviolet band produced a sudden increase of the ionospheric electron density on the daylight hemisphere. The effect of the October 28 X-flare on the slant TEC (STEC) for three stations, covering a wide range in longitude and latitude, is shown in Fig. 1. Indeed, the ionospheric refraction computed from GPS double-frequency carrier phase measurements experienced a sudden increase of about

[1]http://esamultimedia.esa.int/docs/egnos/estb/esaEG/estb.html

[2]http://sohowww.nascom.nasa.gov

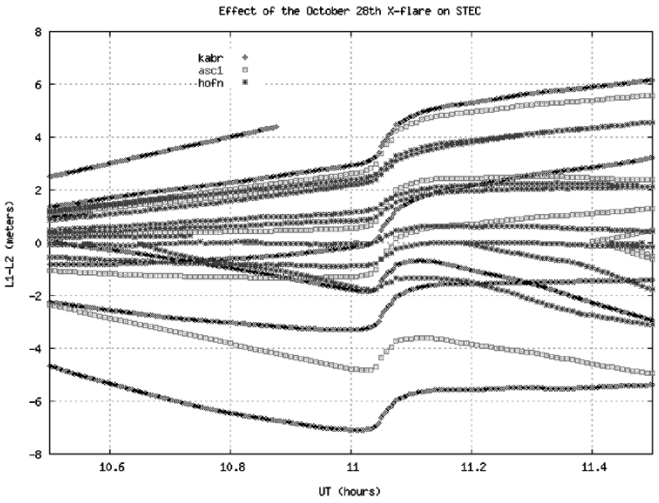

Fig. 1. STEC variations when the X-flare burst happens (about 11 UT of October 28). The STEC has been computed from phase measurements (L1–L2) of satellites in view from three stations in the daylight hemisphere: asc1 (longitude $= 346°$, latitude $= -8°$), hofn (longitude $= 345°$, latitude $= 64°$), and kabr (longitude $= 35°$, latitude $= 33°$).

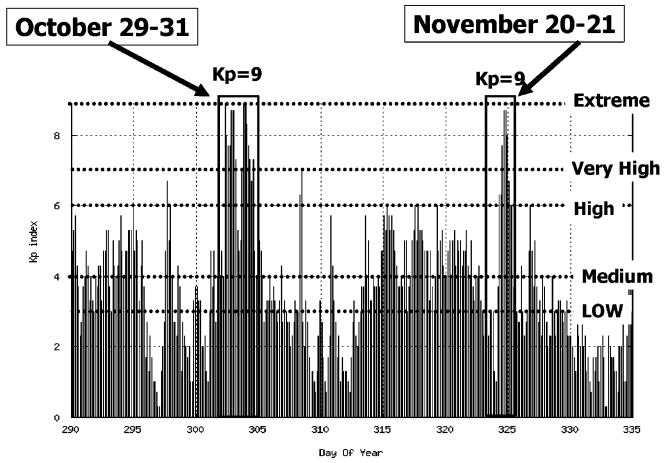

Fig. 2. Kp index from October 17 (DoY 290) up to December 1 (DoY 335) of 2003.

2 m of L1–L2 delay (3 m in L1 delay) after 11 h UT, coinciding with the X-flare detection.

Associated with the X-flare, a coronal mass ejection occurred, which sent a large particle cloud impacting the Earth's magnetosphere about 19 h later, on October 29. Subsequent impacts were still occurring several hours later. This material interacted with the Earth's magnetosphere, and a storm enhancement density (SED) [1] coming from North America affected the northern latitudes in Europe above 50° north in latitude. Extra large gradients of TEC associated with this phenomenon were also produced, degrading the integrity and performance of GPS positioning.

During the storm, large values of the planetary Kp index (3-h index of geomagnetic activity) were experienced, reaching maximum levels of Kp $= 9$ during the most severe periods on October 29 and 30 (see Fig. 2).

In Fig. 2, a second peak of extreme value of Kp $= 9$ is also shown on November 20, 2003. This corresponds to another large ionospheric storm that produced two enhanced regions reaching Europe from northern and middle latitudes and affecting all sites in the European networks. In the case of the November Storm, the X-flare was produced on November 18 by the same group of sunspots (about one solar rotation later), but in this case, the flash was not directed toward to the Earth as was the case of the October one.

The impact of the October and November 2003 storms on the ESTB performance is analyzed in this work in both the position and signal-in-space domains.

This study has been carried out within the ESTB Data Collection and Analysis campaign of Eurocontrol, where several European centers have been collecting and analyzing ESTB data since January 1, 2002. During two consecutive years, 24 h ESTB datasets have been collected every week from Thursday 10 UT to Friday 10 UT and the ESTB performance was analyzed in both the position and the signal-in-space (SIS) domains. In particular, since the end of August of 2002, any potential anomaly detected in the collected datasets in Barcelona was studied in detail to identify the potential cause: orbits and clocks, ionosphere, environment, or processing software. This study revealed that although the ionospheric algorithm implemented in the ESTB is rather simple, the ionosphere was not an important source of integrity problems for the ESTB: only in two cases, September 12, 2002 and August 21, 2003 were the anomalies related to the ionospheric corrections.[3] Only the two extreme events of October 30 and November 20, 2003 produced wide regional degradations such as those analyzed in this paper.

It must be pointed out that this study is only devoted to analysis of the ESTB performance, not the performance of the "true" final EGNOS system, i.e., the professional safety of life system, conceived with all safety considerations and design implications.

The European Space Agency has analyzed the performance of the final EGNOS system for the October and November 2003 storms through postprocessing with the true EGNOS algorithms the worst ionospheric conditions simulated by the Ionospheric Expert team (IET scenario 5; see [2]). Montefusco *et al.* [2] indicate that the obtained results show that the EGNOS system (whose ionospheric algorithms are completely different from those of the ESTB), showed excellent performance, with full integrity and good availability, for the same stormy days of October and November 2003.

II. ESTB Signal-in-Space and Data Processing

The ESTB became operational in January 2000, broadcasting a MOPS [3], [4] compliant SIS through INMARSAT Atlantic Ocean Region-East (AOR-E), until October 23, 2003, and afterward was available through Indian Ocean Region-West (IOR-W); see Fig. 3.

[3]http://www.eurocontrol.fr/projects/sbas

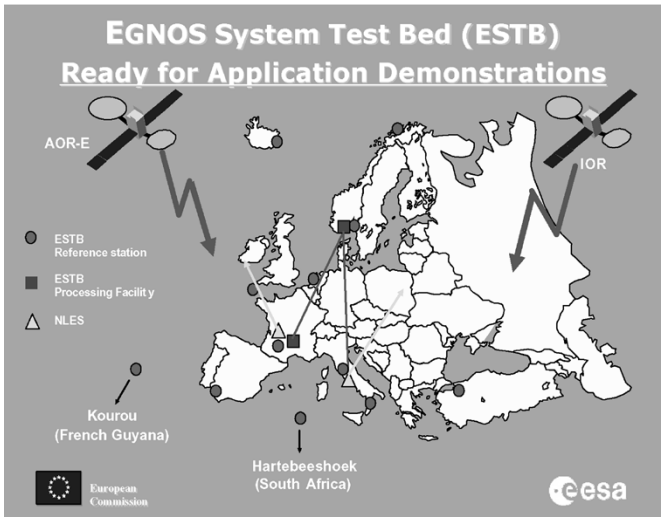

Fig. 3. ESTB architecture and reference stations (RIMS) in circles.

TABLE I
ESTB MODE 2 (FAST) AND IONOSPHERE CORRECTIONS PLUS RANGING

Type	Implemented	Exceptions
0	Yes	With contents of a type 2 message
1	Yes	None
2-5	Yes	None
6	Yes	None
7	Yes	None
9	Yes	None
10	Yes	Fixed parameters
12	Yes	None
17	Yes	None
18	Yes	None
24	Yes	None
25	Yes	Velocity code = 0 and Slow corrections filled to zero.
26	Yes	None
27	Yes	Broadcasted only when testing ESTB outside nominal area and with code conforms to RTCA/Do-229A dated June 08, 1998.
63	No	None

A. ESTB Signal-in-Space During the Storms

During the October and November 2003 storms, the ESTB SIS was broadcast by IOR-W in mode 2 (i.e., fast corrections and ionosphere corrections with GEO Ranging), according to MOPS [4], with contents of a type 2 message in each type 0 message, and with the exceptions given in Table I. Detailed information about ESTB signal schedule can be found at http://esamultimedia.esa.int/docs/egnos/estb/schedule.htm.

B. Data Processing

Several measurement files from GPS receiver networks widely distributed over Europe were used to perform a global monitoring of the ESTB during the storms: The public GPS data servers lox, cddisa, lareg, and geodaf,[4] and the ESTB Post Data Provider (EPPS) server,[5] which contains the measurement files of the ESTB reference stations (RIMS). These files were combined with the GEO data collected from an SBAS receiver, and processed with BRUS (a software package developed by the three first authors [5]), in such a way that an SBAS receiver was emulated at each site. Some datasets were also processed with the software PEGASUS [6] to compare the results. Only the GEO ranging was out of the scope of such emulation, which did not affect the results because the GEO was not monitored by the ESTB at that time.

In order to improve the geographical coverage, sites with a 30-s sampling rate were included in the datasets beside the 1-s ones. Nevertheless, only the 1-s measurement files were taken into account when analyzing the integrity failures. The 30-s measurements were mainly used to help on the accuracy monitoring. Finally, most of the 1-s data files came from the ESTB reference stations used for generating the SBAS message; therefore the best performance should be expected for such stations.

The datasets were processed in the Precision Approach mode, according to MOPS [4], but without applying smoothing to avoid any anomaly masking, and following the data processing strategy applied in the ESTB Data Collection and Evaluation Working Group [7] of Eurocontrol. Although the measurements were not smoothed, the receiver noise was set with the model defined in [4, App. J.2.4] for the steady-state when the time constant is 100 s, and assuming the worst case signal reception conditions (i.e., $\sigma_{\mathrm{noise,GPS}} = 0.4$ m and $\sigma_{\mathrm{noise,GEO}} = 1.8$ m).

C. Protection Levels and Integrity

Integrity is the system's ability to provide warnings to the user when the system is unavailable for a specific operation. The SBAS system provides the users with integrity information to compute the protection levels [horizontal and vertical protection levels (HPLs and VPLs)], which represent an upper bound on the position error.

For each operational mode, alert limits (ALs) against which the user has to compare its protection levels are defined (ICAO's global navigation satellite system standards and recommended practices),[6] and the system is declared as unavailable when the protection level is greater than the alert limit. If the system is available and the position error is not bounded by the protection level, thence the event is considered as a HPL or VPL failure, since the protection level is always supposed to be an upper bound on the position error. In such a case, the event is declared as hazardously misleading information (HMI) if the position error exceeds the alert limit (which suppose an integrity risk), or as misleading information (MI) if the alert limit is not exceeded (see Fig. 4).

[4]Public GPS data servers: lox.ucsd.edu (lox); cddisa.gsfc.nasa.gov (cddisa); lareg.ensg.ign.fr (lareg); geodaf.mt.asi.it (geodaf)

[5]The ESTB Post Data Provider Server (Account and Password is Needed): http://estbsrv.gdiv.statkart.no.

[6]For more information: "Draft SARPS for satellite navigation systems," ICAO GNSS Panel, Montreal.

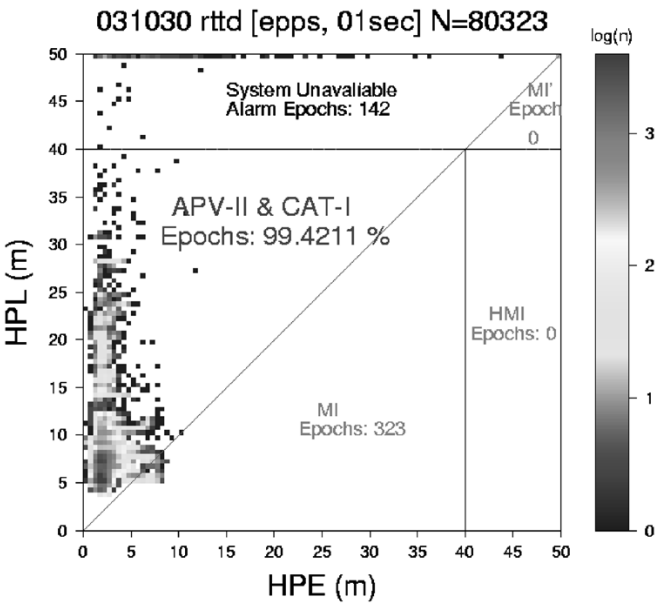

Fig. 4. Stanford plot for the horizontal component at the station of Rotterdam (24 h data for October 30, 2003). The horizontal axis is the horizontal position error (HPE) and the vertical axis the HPL. The alert limit is also shown in the plot as horizontal and vertical lines at 40 m. The MIs corresponds to the bins below the diagonal of the square and below the alert limit: 323 epochs in the figure. No HMIs occurs in this data.

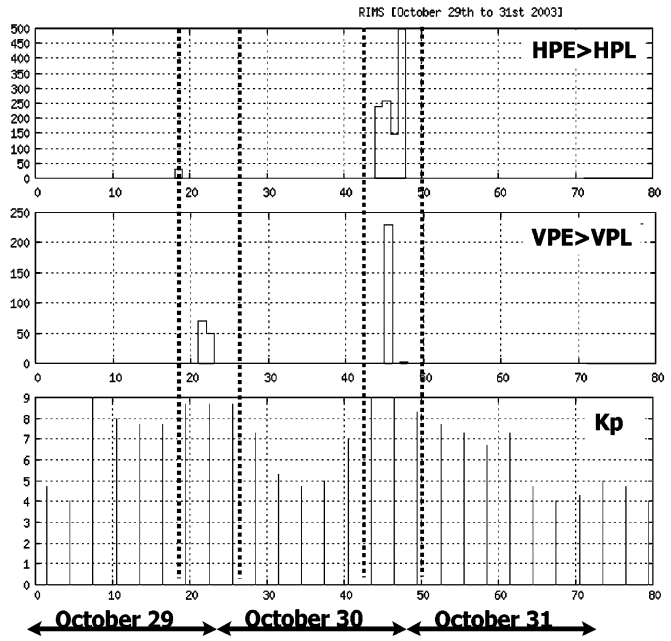

Fig. 5. Relation between the number of events with XPE $>$ XPL in (top) the horizontal and (middle) vertical error components, and the Kp index during the last three days of October 2003. It includes the data files available from European ESTB RIMS at a 1-s sampling rate (except Malaga RIMS). The vertical scales range between 0–500 for the horizontal component, 0–250 for the vertical component, and 0–9 for the Kp index. No HMIs were experienced at such RIMS for the horizontal APV-II and Cat-I (HAL $=$ 40 m) and Vertical APV-II (VAL $=$ 20 m).

III. ESTB Performance During the October and November Superstorms

A. Impact of the Storms in the ESTB Integrity

The impact of the storms on the integrity, measured as the number of protection level failures (XPE $>$ XPL) in the horizontal and Vertical components, and its relation with the Kp index is shown in Figs. 5 and 6 (October and November storms, respectively) for the European RIMS. All available European RIMS stations, with measurements at 1-s intervals, have been included in these plots, except the Malaga RIMS (south of Spain) in the October storm. No HMIs were experienced in such RIMS in the Horizontal APV-II and Cat-I (HAL $=$ 40 m) and Vertical APV-II (VAL $=$ 20 m), i.e., no integrity failures for such navigation modes. As it is shown, there is a great correlation in time between the periods with extreme values of Kp and the number of events with XPE $>$ XPL observed during both storms.

The ESTB performance in three European stations for the October 30 storm is compared in Fig. 7. Two stations are located in The Netherlands (Delft and Rotterdam -Rott-), with about 5 km of base-length, and the other in Spain (Barcelona -BCN-) about 1200 km away. As can be seen in the second column plots, the HPE in Rotterdam [Fig. 7 (top)] and Delft [Fig. 7 (bottom)] shows a similar signature, with two peaks between 21 and 22 UT and 22 and 23 UT (the plot of Rotterdam is noisier than the Delft because many satellites were unavailable in the available RINEX file). These peaks, which are not bounded by the HPL, are responsible for the MIs at such sites. On the other hand, the receiver at Barcelona (below left) shows

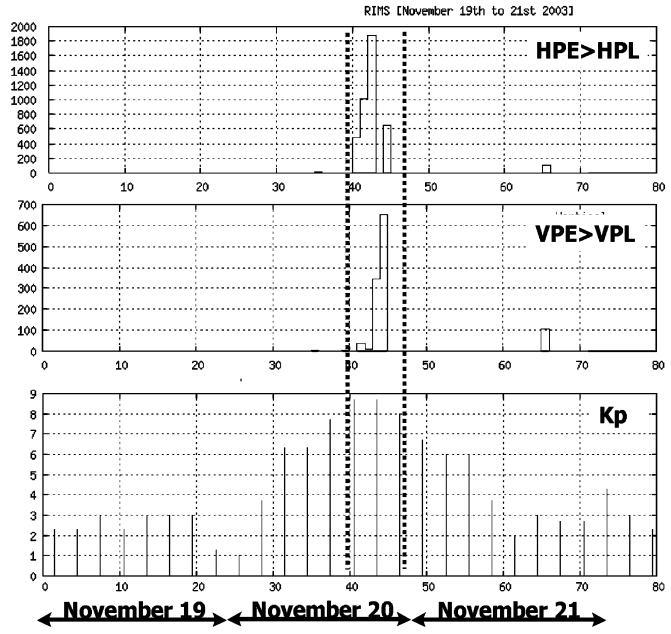

Fig. 6. Plots similar to Fig. 5, but for November 19–21, 2003. All available RIMS stations in Europe have been included in the analysis.

a similar pattern for the protection levels as Delft, but its navigation solution shows nominal values, always bounded by the protection levels. The HPE peaks at the Delft and Rotterdam sites were related with the large gradients of TEC, affecting the north of Europe at the end of October 30, due to a density enhancement coming across from North America (see Fig. 11).

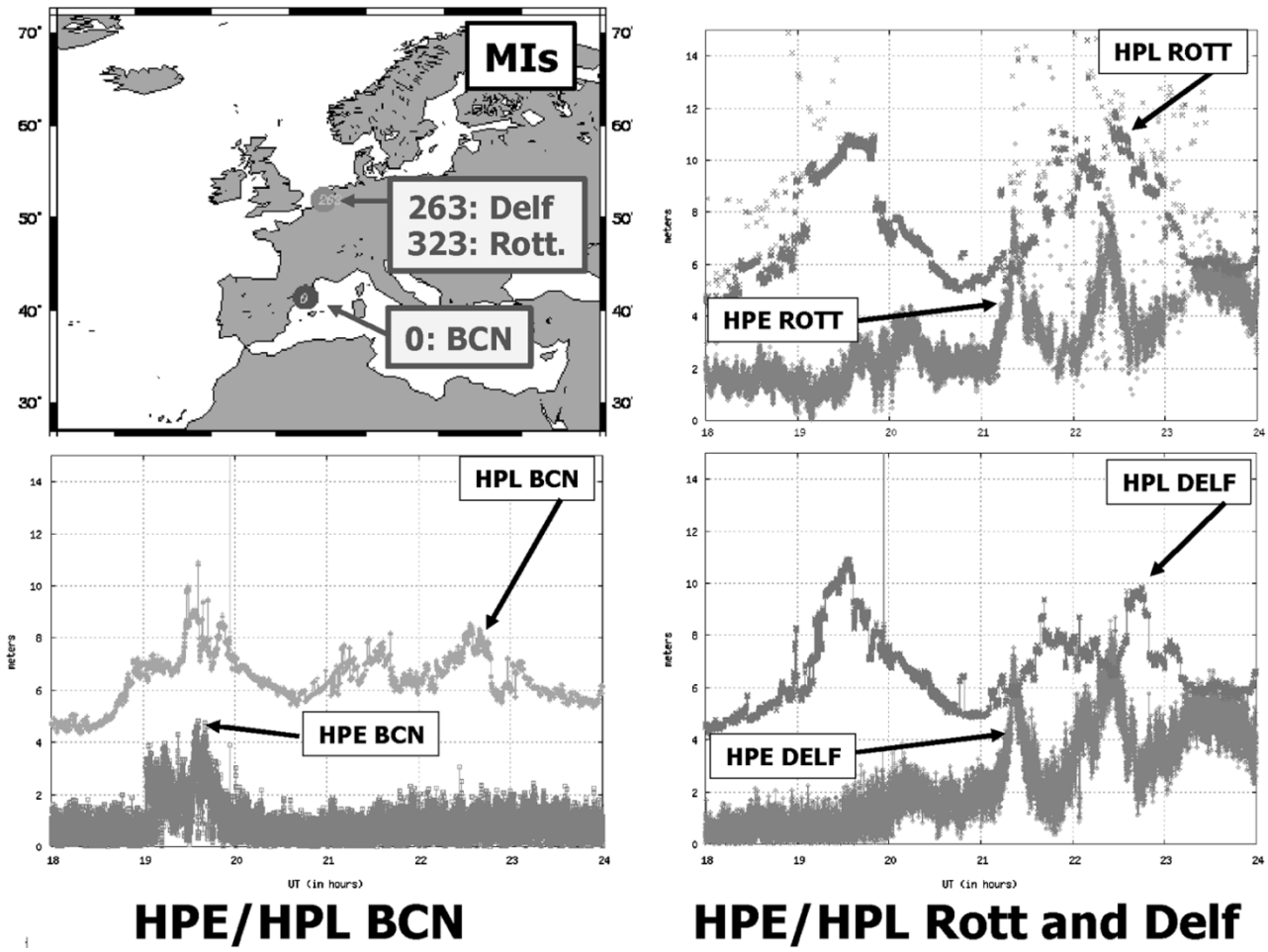

Fig. 7. Comparison of ESTB performance in three sites for the October 30, 2003 storm, from 18 to 24 UT: Barcelona (BCN), Delft (DELF), and Rotterdam (ROTT). (First column, top) Number of MIs, which are similar in Delft and Rotterdam. (Second column) Horizontal position error and protection level (HPE/HPL) in (top) Rotterdam and (bottom) Delft, with the same signature. (Bottom left) Position error and protection levels for Barcelona. Notice the different behavior between the HPE in Barcelona and Delft or Rotterdam due to the storm. In the HPE/HPL plots, the horizontal scale ranges from 18–24 UT, and the vertical one from 0–15 m.

The November 20 storm presented two enhanced regions reaching Europe from northern and midlatitudes (see Fig. 12) that affected all the sites in the analyzed European networks. And in particular, the above mentioned sites of Delft, Rotterdam and Barcelona, showed similar degradations of the ESTB performance.

In Fig. 8 (top), the HPE and HPL, computed from ESTB data, are shown together with the standalone GPS solution for the station of Delft $(\text{lon} = 4°5, \text{lat} = 52°)$. The figure corresponds to the time interval from 19 h to 22 h UT of October 30. This period contains the first large peak in the HPE shown in Fig. 7. Notice that, although the ESTB solution is more accurate than the GPS standalone, both navigation solutions show the same peak in the position error.

The following plots of Fig. 8 show the ionospheric refraction computed from double-frequency GPS code and phase measurements for several satellites (PRN 15, 16, 18, and 02) used in the navigation solution. The curves have been aligned with the STEC computed from the ESTB broadcast data in order to compare their shapes. The ESTB ionospheric bound, i.e., the user ionospheric range error (UIRE), is also given in the figure.

The plot with the location of the satellites in view is shown at bottom right of Fig. 8. And, at bottom left, a map is provided to show the discrepancies between the ESTB vertical delays (TEC) and the TEC computed from the Global Ionospheric Maps (GIMs) provided by International GPS Service (IGS) [8]. The ionospheric Pierce points (IPP) for the satellites in view are also included in this map. Under normal conditions, the accuracy of TEC computed from the IGS GIMs over Europe is about 3 TECUs (less than 0.5 m of L1). Under storm conditions, the accuracy is worst, but they can still be used as a rough reference to provide a first glance of error distribution of the ionospheric determinations.

As can be seen in Fig. 8, the peak in the HPE also appears in the ionospheric refraction plots of satellites PRN15 and PRN18 computed by GPS double-frequency code (P2–P1) and phase measurements (L1–L2). Such peaks have a duration of about 10–15 min and involve an increment of the ionospheric delay of about 10 m in L1. This fast variation of the ionospheric refraction is not followed by the ESTB STEC (and also the UIREs are not inflated properly), degrading the accuracy of the navigation solution. Nevertheless, as can be appreciated in the Figs. 8 and 9,

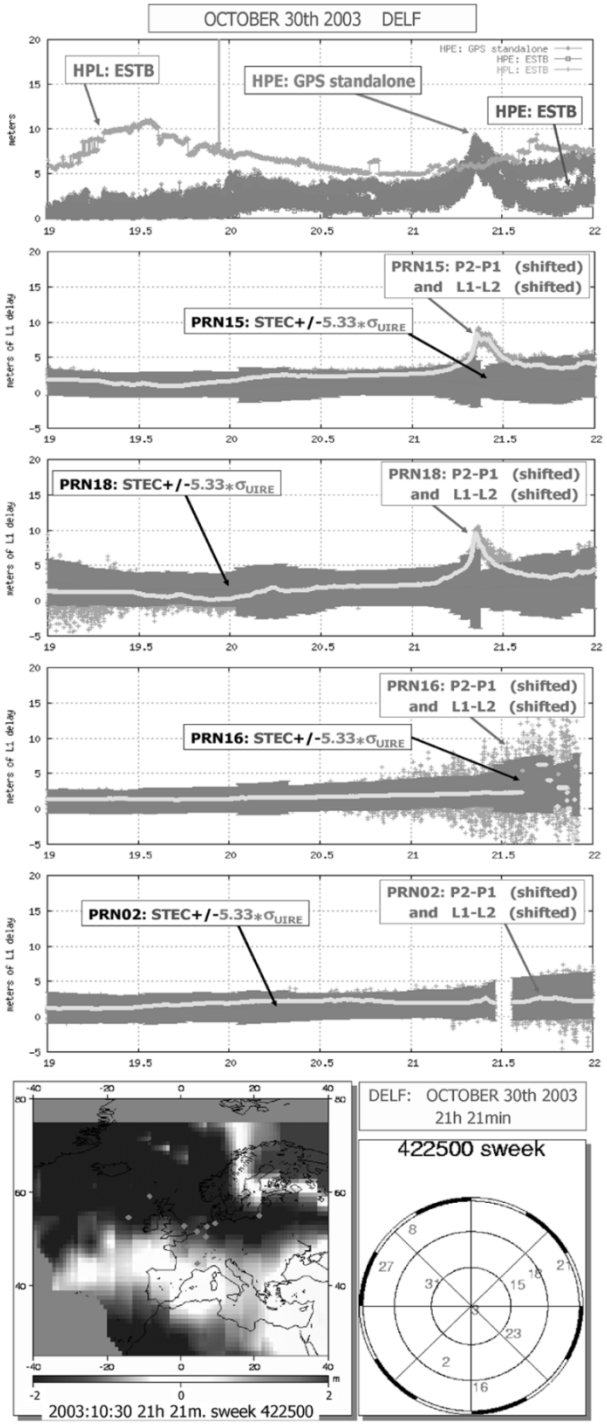

Fig. 8. Delft (Netherlands), October 30, 2003. (Top) GPS standalone HPE and the ESTB HPE/HPL, from 19–22 UT. (Next four rows) The ESTB STEC with the confidence bound (UIRE) is compared with the ionospheric refraction computed from code (P2–P1) and phase (L1–L2) measurements for satellites PRN 15, 18, 16, and 02. (Bottom left) Map with the discrepancies between the ESTB and IGS vertical delays (in meters of L1 delay, color palette saturating at ± 2 m of L1). The IPPs are also given in the map. (Bottom right) Sky plot with the satellites used in the navigation solution to show the geometry of the satellites in view from Delft, and to identify the IPPs in the previous map (notice that the projection is quite different).

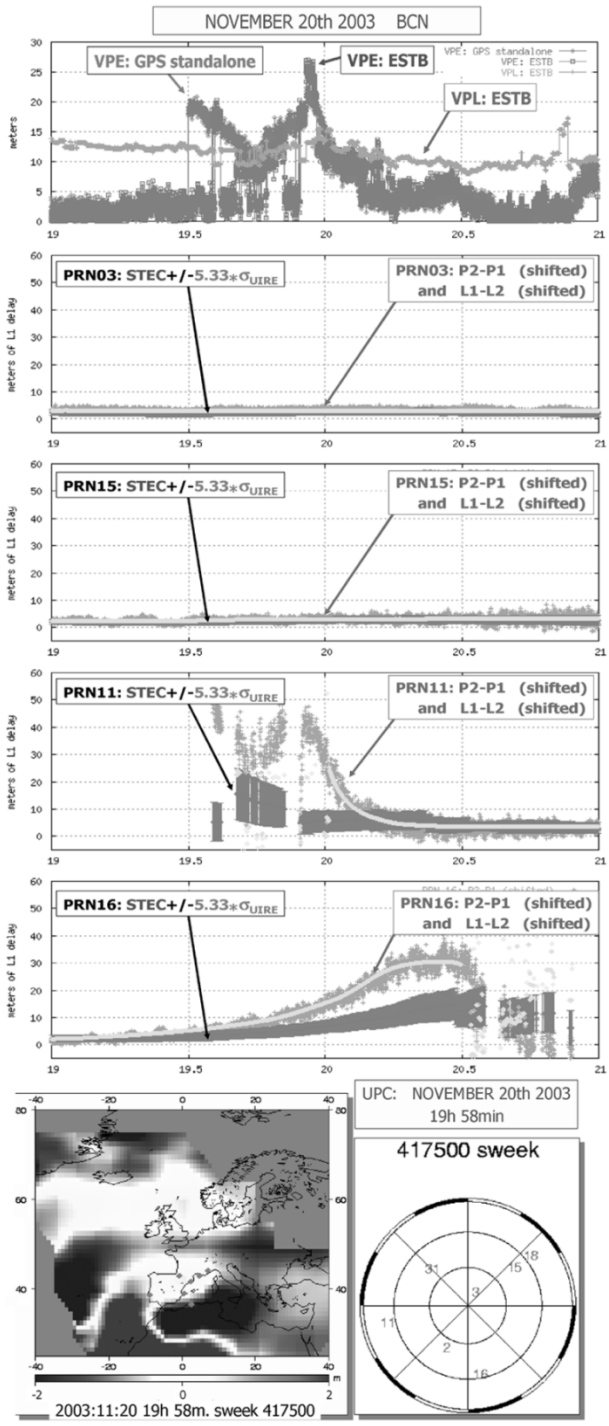

Fig. 9. Similar plots as in Fig. 8, but for Barcelona on November 20. 2003, from 19–21 UT. The vertical position error and protection level are displayed in the figure above instead of the horizontal ones. Different scales are also used in Fig. 8.

there is an increase of the UIRE by the time of the peaks in XPE, which means that the system is reacting somehow to increase the error estimate, but it is not enough to overbound the real error.

On the other hand, not all the satellites in view are affected in the same way by the ionospheric TEC gradients. For instance, no peaks appear when analyzing the ionospheric refraction plots of satellites PRN02 and 16, which show very flat patterns over the 3 h.

It must be pointed out that the error budget is composed not only of the ESTB broadcast information, but also the interpola-

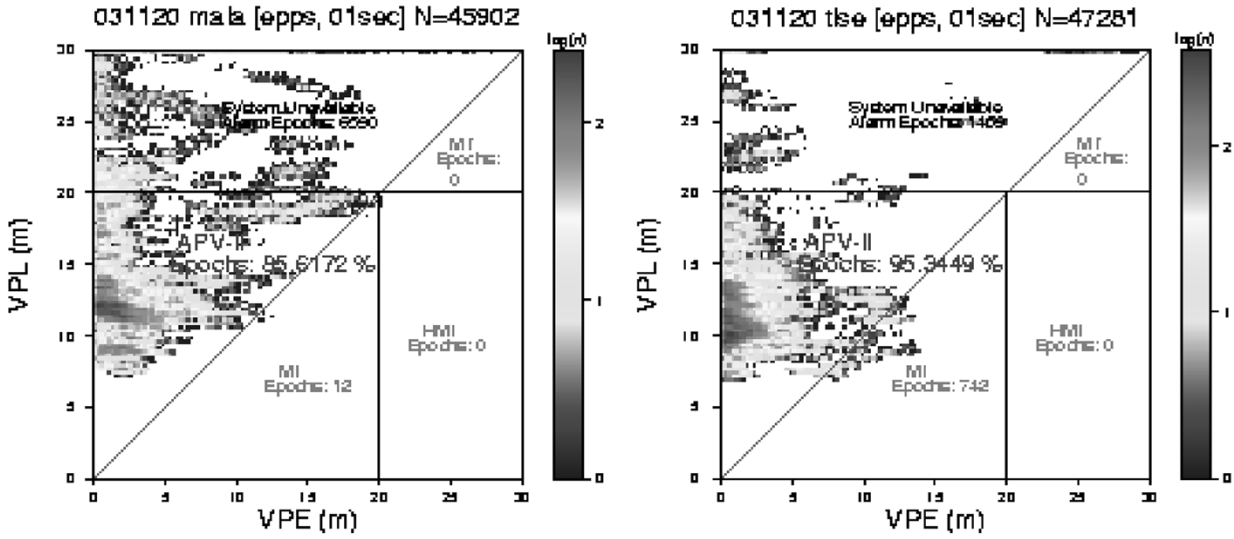

Fig. 10. Vertical APV-II Stanford plots for (left) the Malaga and (right) Toulouse RIMS. The datasets are from 10–24 UT of November 20, 2003. No HMIs are experienced in these two RIMS. The horizontal and vertical scales range from 0–30 m. VAL $= 20$ m.

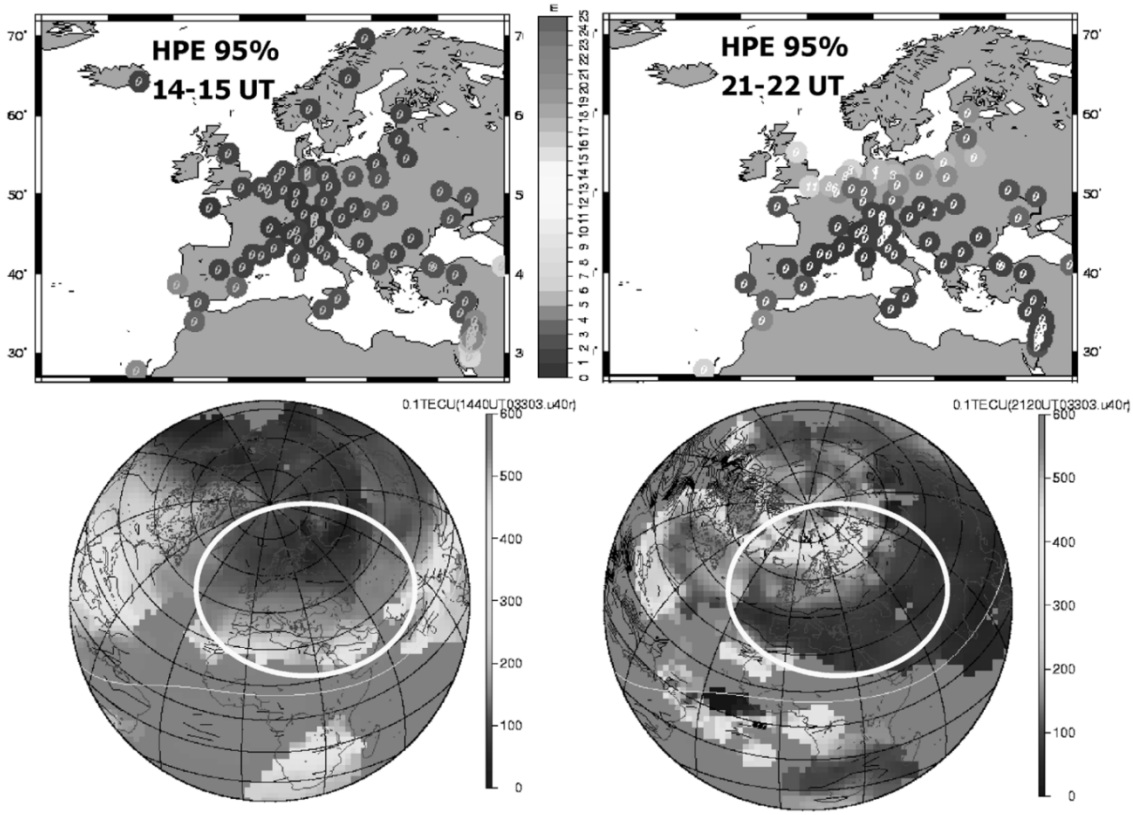

Fig. 11. Two snapshots of ESTB performance (horizontal accuracy: 95th percentile) and total electron content, on October 30, 2003. The color scale for HPE is given in meters, ranging from 0–25 m, and in tenths of TECUs (1TECU $= 16$ cm of L1 delay), from 0–600 tenth of TECUs, for the TEC. All available stations, with measurements at 1 and 30 s, have been used in this plot. The TEC images have been generated from the UPC Global Ionospheric Maps final product.

tion algorithm (defined by MOPS [4]) and also the refresh rate (it was every 3 min on average).

From the scatter plot and the map at the bottom of Fig. 8, it can be seen that the satellites PRN 15 and 18 have IPPs close together, which are located in a region with large discrepancies between the ESTB and the IGS TEC determinations. However, the other satellites, PRN 02 and 16, are located in another region with lower discrepancies. It must be pointed out that the discrepancies map does not provide the actual error of the ESTB TEC. It only provides the discrepancies between the ESTB and IGS TEC determinations, and both could be biased, at the same time. The regions in which large discrepancies appear can be viewed

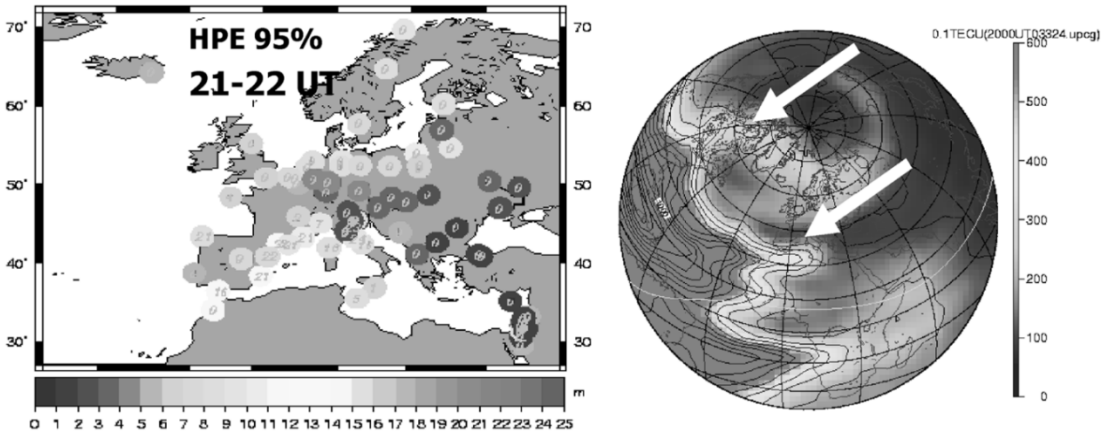

Fig. 12. ESTB performance (horizontal accuracy: 95th percentile) and total electron content, on November 20, 2003 between 21 and 22 UT, the period with worse global performance. The color scale for HPE is given in meters, ranging from 0–25 m, and in tenths of TECUs (1TECU $=$ 16 cm of L1 delay), from 0–600 tenth of TECUs, for the TEC. All available stations, with measurements at 1 and 30 s, have been used in this plot. The TEC images have been generated from the UPC Global Ionospheric Maps final product. The white arrows point to the main electron content perturbations.

as an indicator of the areas that are more difficult to model due to fast variations or big gradients of TEC. Regions with low discrepancies will be those where the determinations are probably more accurate. This is compatible with the absence of the peak in the STEC of satellites PRN 02 and 16, which pierce a region with low discrepancies.

Similar results as in the October's storm can be seen for the November's storm in Fig. 9. The plots correspond to a receiver located in Barcelona $(\text{lon} = 2^\circ, \text{lat} = 41^\circ)$. In this case, the vertical performance is shown (VPE and VPL) instead of the horizontal, because this is the component most degraded. In this case the satellites with the largest STEC errors are PRN 11 and 16, reaching values of up to 45 and 15 m, respectively on L1, with respect to the GPS aligned code and phase measurements (P2–P1 and L1–L2). As in the October storm, the errors in the ESTB ionospheric values for these satellites are not bounded by the UIRE, significantly degrading the navigation solution.

This produces a large number of MIs due to the PRN 11 satellite. In this case about 20 UT, the VPE rises above 20 m (the VAL for APV-II) and, as the VPL $<$ VAL, HMI events occur. Such HMIs do not appear in the analyzed European RIMS, in particular, in Toulouse or Malaga, the closest ones to Barcelona (see Figs. 10 and 14).

On the map at the bottom of Fig. 9, it can be seen that all the satellites in view from the receiver in Barcelona pierce a region with low discrepancy values between ESTB and IGS TEC, except PRN 11 and 16 which are located in the border of a region with large gradients. Finally, and according to the discrepancies map, again most European sites observed one or more satellites in the large mismodeling regions (where the ESTB or the IGS TEC determination, or both are degraded due to the fast TEC variations and large gradients). This explains the global degradation of the navigation solution at the different sites (see Fig. 12).

Thence, the large gradients and fast variations of the ionospheric electron content due to the SED in the northern regions introduced an important mismodeling in the computation of the ionospheric corrections by ESTB Central Processing Facility (CPF), which was not able to react with accurate enough ionospheric corrections to compensate for the effects of the storm. Also the integrity data broadcast to compute the protection levels was not tuned enough to bound the ionospheric error, which exceeded by far the UIRE values, as can be seen in the plots of Figs. 8 and 9. As a consequence many MIs occurred at that time.

B. Impact of the Storms on the ESTB Accuracy

As it has been shown in previous sections, the October's storm affected mainly to the European stations at high latitudes, especially at the end of October 30, 2003. In Fig. 11 two snapshots of the horizontal accuracy (95th percentile) and the total electron content (TEC) can be seen for two time intervals of 1 h.

The first one, on the left, corresponds to a quiet period in the afternoon, between 14 to 15 UT, in which the accuracy is kept within the nominal values, with degradation in the borders of the coverage area, in particular in the southeast (Middle East) and southwest (Canaries Islands). The second one, on the right, corresponds to a very active period, between 21 to 22 UT, in which the SED reached the north of Europe, degrading the accuracy of ESTB at latitudes above 50°. These large errors (more than 5 m) were experienced until 01 UT of October 31, 2003.

In the case of the November 20, 2003 storm the degradations of the accuracy affected all of Europe. A snapshot of the horizontal accuracy (95th percentile) and the global TEC map are shown in Fig. 12 for a very active period of the night, between 21 and 22 UT, where two enhanced regions reach Europe in the north and southeast, producing large gradients of TEC and degrading the accuracy of ESTB in most of the European stations.

The navigation system error (HPE and VPE) and protection levels (HPL and VPL) as a function of time during the last 6 h of October 30, 2003 are shown in Fig. 13 for eight different

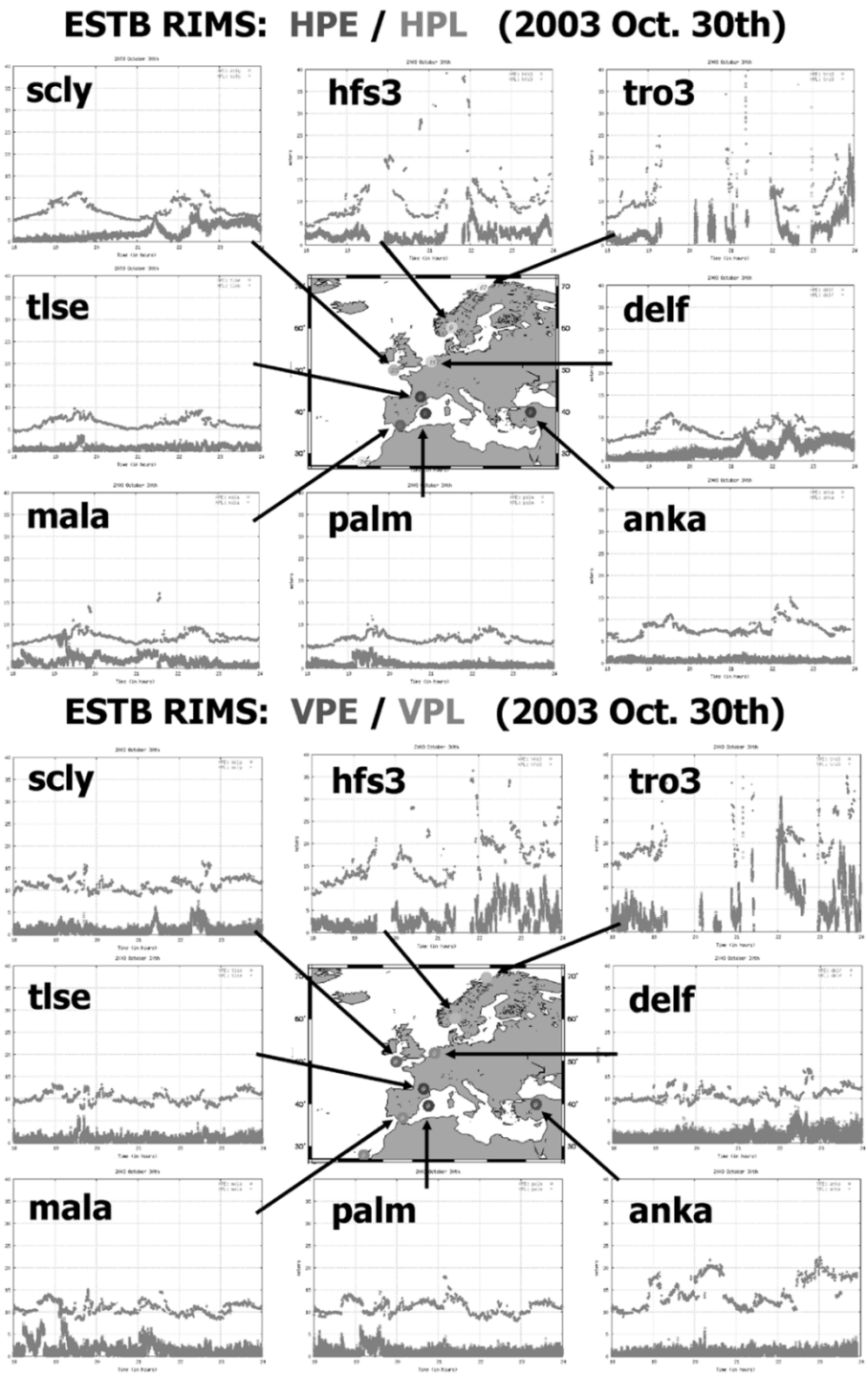

Fig. 13. Navigation system error and protection levels at eight ESTB RIMS during the last 6 h of October 30th. (Top) HPE/HPL and (bottom) VPE/VPL. The horizontal scale ranges from 18–24 UT, and the vertical one from 0–40 m. After noon, the positioning error increase in all the sites above 50° of latitude, especially in the horizontal component, and the protection level does not bound the positioning error, raising the MIs (see tro3 at 22 UT). The other sites below 50° do not present MIs, except in Mala (south of Spain), but about 19 UT, which are related with the location of this site, close to the border of coverage area. Note: the station delf is plotted instead of the RIMS rttd.

RIMS around Europe (the RIMS of Rotterdam -rttd- has been replaced by the station of Delft -delf-, 5 km away, due to the lack of data in the RINEX file of rttd). Similar protection levels are seen for all the RIMS, except those with latitude greater than 60° (tro3 and hfs3) where the ionospheric corrections were not always available and no navigation solution was provided at these times. Nevertheless, large errors are found in the RIMS above 50°, scly (UK) and delf (or rttd) (Netherlands), due to the storm. It should be noted that a similar pattern of HPE and HPL is seen at the sites scly and delf (or rttd), about 800 km away. The protection levels do not bound the error of the ionospheric determinations in the region affected by the storm. In

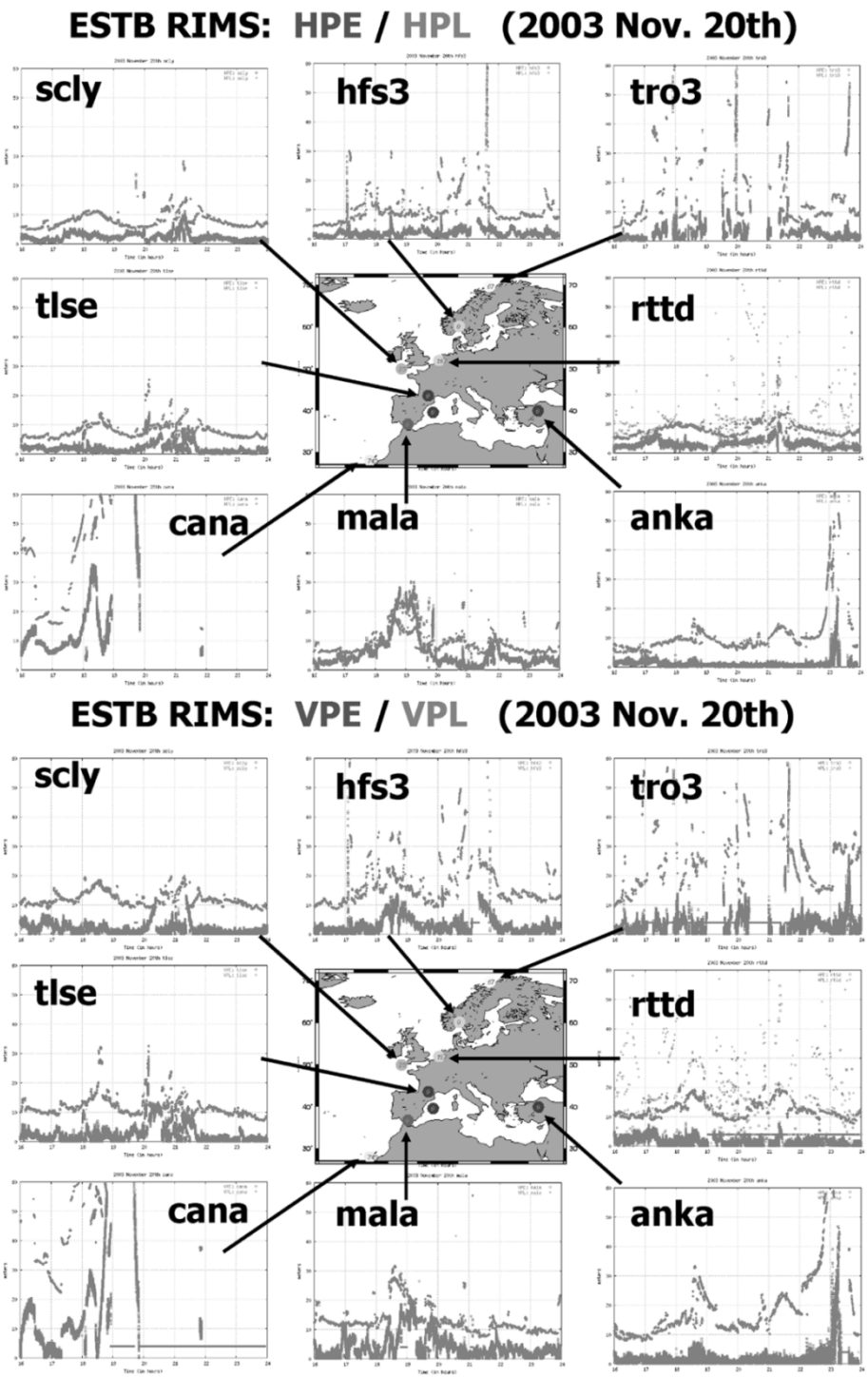

Fig. 14. Navigation system error and protection levels at eight ESTB RIMS during the last 6 h of November 20. (Top) HPE/VPL and (bottom) VPE/VPL. The horizontal scale ranges from 18–24 UT, and the vertical one from 0–60 m. After noon, the positioning error increase in all the European sites, in the horizontal and vertical components, and the protection level does not bound the positioning error, raising the MIs.

the "mala" RIMS, MIs appear around 19 UT, but not after 21 UT as in the stations above 50° of latitude. The MIs in "mala" were also related to the ionosphere, but not with the SED that appeared in the north of Europe after 19:30 UT. It must be taken into account that this station is located in the south of the coverage area and its measurements are affected by the ionospheric equatorial gradients.

Similar results, but affecting all the stations in Europe, are shown for November 20, 2003 in Fig. 14. In this case, the degradation of the accuracy affects all the European sites.

IV. Conclusion

Two severe geomagnetic storms were experienced on October 29–31 and November 20, 2003, degrading the ESTB perfor-

mance in Europe. Such storms reached maximum levels of geomagnetic activity ($\mathrm{Kp} = 9$) during the most severe periods.

The October storm was experienced from the 29th in the afternoon to the beginning of the 31st, with large oscillations on the 30th, and presenting a storm enhancement of density, coming from North America and affecting the northern latitudes of Europe above 50°. The November storm occurred mainly in the afternoon of the 20th and resulted in two enhanced regions reaching Europe from northern and middle latitudes and affecting all sites in the European networks.

The storms have been monitored from a network of GPS receivers distributed over Europe, including the ESTB reference stations. The measurement files have been combined with the SBAS messages gathered from the GEO through an SBAS receiver. They were processed with navigation software in such a way that an SBAS receiver was emulated at each site.

The ESTB performance has been analyzed during both storms in both the signal-in-space and in the position domains. In the SIS domain, large discrepancies appear when the ESTB slant total electron content is compared with the ionospheric refraction computed from double-frequency GPS code and phase measurements. Only the shape of such determinations is compared, which is enough to illustrate the magnitude of the errors that are not bounded by the confidence values and thus result in the MIs. A map with the discrepancy between the ESTB and IGS vertical delays (TEC) has also been generated to help the analysis of the geographical distribution of the satellites that contribute to the MIs.

In the position domain, the accuracy of the navigation solution is significantly degraded in the horizontal and vertical components, resulting in errors of 10 m or more at some sites. In spite of the occurrence of a large number of MIs, no integrity failures (HMIs) were experienced at the European RIMS for the Horizontal component (APV-II and CAT-I) or the vertical one up to APV-II during the analyzed stormy periods. However, some HMIs were found in November 20, 2003, in Barcelona, Spain, for vertical APV-II. On the other hand, those MIs were highly correlated in time with the periods of extreme Kp values during both storms.

The ESTB is a simple prototype of the final European SBAS system EGNOS with several limitations: it is an accuracy system with no integrity intended, no safety processor, no storm gradient detectors, and no integrity check and runs with a simple ionospheric algorithm. In this context, and considering the high strengths of the analyzed storms, it can be concluded that the ESTB system was performing rather well in such difficult conditions.

Finally, it is to be noted that the European Space Agency has analyzed the performance of the final EGNOS system for the October and November 2003 storms (IET scenario 5), through postprocessing with the true EGNOS algorithms. Montefusco *et al.* [2] indicate that the obtained results show excellent performance, with full integrity and good availability.

ACKNOWLEDGMENT

The authors would like to thank the IGS community for providing the ground receiver data.

REFERENCES

[1] J. C. Foster, P. J. Erickson, A. J. Coster, J. Goldstein, and F. J. Rich, "Ionospheric signatures of plasmaspheric tails," *Geophys. Res. Lett.*, vol. 29, no. 13, p. 1623, 2002. DOI: 10.1029/2002GL015067.

[2] C. Montefusco, J. Ventura-Traveset, B. Arbesser-Rastburg, F. Froment, D. Flament, E. Tapias, S. Radicella ICPT, and R. Leitinger, "Assessment of EGNOS performance in worst ionosphere conditions (October and November 2003 storm)," presented at the *Eur. Navigation Conf. GNSS*, Munich, Germany, 2005.

[3] RTCA, "Minimum operational performance standards for GPS/WAAS airborne equipment," Radio Tech. Commiss. Aeronautics, Washington, DC, Do 229A, Jun. 1998.

[4] RTCA, "Minimum operational performance standards for GPS/WAAS airborne equipment," Radio Tech. Commiss. Aeronautics, Washington, DC, Do 229B, Oct. 1999.

[5] M. L. Hernández-Pajares, J. M. Juan, J. Sanz, X. Prats, and J. Baeta, "Basic research utilities for SBAS (BRUS)," presented at the *V Geomatics Week*, Barcelona, Spain, 2003.

[6] Eurocontrol, "PEGASUS interface control document," Eurocontrol, Bretigny, France, Doc. No.: PEG-ICD-01, Issue E.

[7] "Data Collection Report Proposed Template," EEC GOV Working Group Is.1 Rev. 1.

[8] M. Hernandez-Pajares, "IGS ionosphere WG position paper: Present and future activities," presented at the *IGS Technical Meeting*, Bern, Switzerland, Mar. 2004.

Manuel Hernández-Pajares is currently with the Department of Applied Mathematics and Telematics, Universitat Politècnica de Catalunya, Barcelona, Spain. He started working on GPS in 1989 and is currently focused on the area of GPS ionospheric tomography, neural network algorithms, and precise radionavigation.

J. Miguel Juan Zornoza is currently an Associate Professor with the Department of Applied Physics, Universitat Politècnica de Catalunya, Barcelona, Spain. His current research interest is in the area of GPS: tomography of the ionosphere, data processing strategies, and subdecimeter navigation.

Jaume Sanz Subirana is currently with the Department of Applied Mathematics and Telematics, Universitat Politècnica de Catalunya, Barcelona, Spain. He is working on GPS processing software, ionospheric tomography with GPS data, and real-time precise positioning.

Richard Farnworth is currently with the Eurocontrol Experimental Centre, Bretigny, France. He is Head of the satellite navigation activities managed from within the Navigation Domain of Eurocontrol and is responsible for research projects related to the application of satellite navigation in civil aviation.

Santiago Soley is working through his cofounded company PILDO Labs S. L. as a consultant for the Eurocontrol Navigation Domain at their Experimental Centre, Bretigny, France, giving technical support in all related activities to GNSS-1 operational validation, and the introduction of GNSS systems for civil aviation.